J. Phys. Chem. A **2003,** *107,* 9189−9196

Gas-Phase Reactions between Silane and Ammonia: A Theoretical Study

Shao-Wen Hu,* Yi Wang, Xiang-Yun Wang, Ti-Wei Chu, and Xin-Qi Liu

Department of Applied Chemistry, College of Chemistry and Molecular Engineering, Peking University, Beijing, China 100871

Received: June 13, 2003; In Final Form: August 8, 2003

Gas-phase reactions between silane (SiH_4) and ammonia (NH_3) were investigated using ab initio calculations at the CCSD(T)/6-311++g**//MP2/6-31+G* level. Within the energy range of 180 kcal/mol, we located 34 equilibrium and 23 transition states on the potential energy surfaces of the Si−N−H systems. The initially weakly bonded molecular complex H_3N-SiH_4 eliminates the first hydrogen molecule (H_2) to form the Si−N bond three ways. The first route is through a dihydrogen-bonded transition state, over a barrier of 49.31 kcal/mol, leading directly to the most stable product silylamine (H_2N-SiH_3). The second route is through SiH_4 dissociating into SiH_2 and H_2, over a barrier of 57.47 kcal/mol, leading to the dative-bonded silylammonia complex H_3N-SiH_2. The third route is through a stepwise atomic dissociation and radical formation process, over a barrier of 131.21 kcal/mol, also leading to H_3N-SiH_2. With more energy, both H_2N-SiH_3 and H_3N-SiH_2 are liable to further H_2 or H elimination, leading to smaller species including molecules H_2N-SiH, $HN-SiH_2$, H_3N-Si, HNSi, and HSiN and radicals H_2N-SiH_2, H_3N-SiH, H_2N-Si, and NSi. Dihydrogen-bonded structures are also responsible for lowering barriers in these processes.

I. Introduction

Understanding the mechanisms of gas-phase reactions between silane (SiH_4) and ammonia (NH_3) is the focus of numerous research,[1−14] because the two simple hydrides are widely used as source gases in chemical vapor deposition (CVD) producing solid silicon nitride,[15−22] a material having special properties.[23−26] Experiment[1] shows that silylamine (H_2N-SiH_3) is the main product of the initial reaction. It is not clear how this product is formed from the original reactants because solid evidence is lacking.[1,2] According to a current view,[1] the first step is SiH_4 dissociating into SiH_2 and H_2 with SiH_2 then inserting into a N−H bond of NH_3. Calculations show that a dative complex H_3N-SiH_2 is another possible intermediate besides H_2N-SiH_3, the insertion product. The transformation between the two species happens over a higher barrier than that for SiH_4 dissociation.[2,27] On the other hand, SiH_2 is known to insert into a Si−H bond of SiH_4 to form Si_2H_6 with almost no barrier.[28−30] Therefore, it seems more reasonable that large amounts of Si_2H_6 and H_3N-SiH_2 instead of H_2N-SiH_3 should be observed following SiH_4 dissociation. In our previous studies,[30−33] we have demonstrated that silane can act either as a Lewis acid or a base depending on the acidity of the species with which it reacts. When it meets with strong Lewis base like NH_3, the reaction pathways should be significantly different from what happens in a pure SiH_4 system. To elucidate reaction pathways that were probably missed in previous studies, we performed a more extended computational exploration on the potential energy surfaces of the Si−N−H system within an energy range of 180 kcal/mol.

II. Calculation Method

The geometry structures were fully optimized at the MP2=Full/6-31+G* level. Transition states were located using synchronous transit-guided quasi-Newton (STQN) methods[34] in combination with stepwise partial optimization along each pathway with one geometric parameter fixed as constant. Frequency calculations were performed following each optimization to obtain the zero point energy (ZPE) and IR spectral data and to characterize all the stationary points located on the potential energy surface. Intrinsic reaction coordinate (IRC) calculations were performed to confirm the relationship of each transition state with its reactant and product. Single point calculations at the MP2=Full/6-311++g** and the CCSD(T)=Full/6-311++g** levels were performed to determine the electronic energies. The relative energies reported in discussion are obtained at the CCSD(T)=Full/6-311++g** level with MP2/6-31+G*-calculated ZPE corrections. For open shell species, the geometry optimization and energy calculation were performed using the same level of theories except that electron spins were unrestricted. The Guassian 98 program package[35] was employed for these calculations.

III. Results and Discussions

Our previous work[30] has shown that geometry optimization for silicon hydride at the MP2/6-31+G* level is in good agreement with experiments and calculations using other theoretical models. For some Si−N−H system, calculations at different levels are reported.[6,36−39] It seems that there is no significant change in geometry parameters and relative energies using higher level theoretical models. In these works the calculated IR data are also compared with available experimental results. Therefore, we did not repeat our geometry optimizations at other levels. Instead, in calculating the pathways, dissociation reactions were treated as isomerization from tight combinations to loosely associated fragments before calculating each part separately. This effort may add accuracy by circumventing basis set superposition error (BSSE). Also, the reaction pathways appear clearer.

---

* Corresponding author. E-mail: sw-hu@163.com.

10.1021/jp035684m CCC: $25.00

TABLE 1: Calculated Electronic Energies (E_e), Zero Point Energy (ZPE), Spin Squared Expectation Values $\langle S^2 \rangle$, Dipole Moments (D), and Eotational Constants of the Si−N−H Systems

		au					Debye			rotational constants[b] (GHZ)		
species	symm[a]	E_e [b]	E_e [c]	E_e [d]	ZPE[b] (kcal/mol)	$\langle S^2 \rangle^d$	D[b]	D[c]	D[d]			
H_3N-SiH_4 (**1**)	C_{3v} (0)	−347.680905	−347.934932	−347.986809	43.67		2.519	2.369	2.449	57.90	4.025	4.025
$H_2N-H_2-SiH_3$_TS (**2**)	C_s (1)	−347.592669	−347.853404	−347.903871	40.93		3.434	3.310	3.500	41.07	10.25	9.674
$H_2N-SiH_3-H_2$ (**3**)	C_s (0)	−347.688852	−347.937984	−347.987542	39.57		1.240	1.128	1.169	17.44	10.30	7.296
H_2N-SiH_3 (**4**)	C_s (0)	−346.544169	−346.776890	−346.818340	32.36		1.175	1.075	1.106	68.64	12.47	12.03
$H_2N-H-SiH_2$_TS (**5**)	C_1 (1)	−346.421573	−346.656101	−346.699217	30.02		2.400	2.255	2.324	72.44	10.89	10.59
H_3N-SiH_2 (**6**)	C_s (0)	−346.485968	−346.717114	−346.762707	34.63		5.638	5.414	5.537	69.57	9.511	9.412
$H_3N-SiH_2-H_2$ (**7**)	C_s (0)	−347.630474	−347.877857	−347.931534	41.67		5.672	5.471	5.593	62.95	5.471	5.458
$H_3N-SiH2-H2$_TS (**8**)	C_1 (1)	−347.578262	−347.836902	−347.891386	41.26		3.213	3.149	3.196	66.19	5.070	5.002
H_3N-SiH_3-H_3 (**9**)	C_1 (0)	−347.546680	−347.790878	−347.838300	37.52	2.001	2.855	2.725	2.814	22.48	3.953	3.570
H_3N-SiH_3 (**10**)	C_s (0)	−347.048307	−347.291032	−347.338445	37.43	0.751	2.877	2.729	2.818	72.59	4.512	4.440
H_3N-SiH_2-H_TS (**11**)	C_s (1)	−346.983689	−347.216789	−347.264101	35.01	0.777	5.783	5.668	5.774	69.56	7.764	7.696
H_3N-SiH_2-H (**12**)	C_s (0)	−346.984473	−347.217053	−347.262673	34.77	0.750	5.588	5.424	5.546	61.35	6.835	6.794
$H_2N-H_2-SiH_2$_TS (**13**)	C_s (1)	−346.961326	−347.211906	−347.257948	34.11	0.751	2.783	2.713	2.937	52.84	10.25	10.20
$H_2N-SiH_2-H_2$ (**14**)	C_s (0)	−347.057538	−347.295203	−347.340920	33.50	0.751	1.399	1.293	1.307	20.17	9.926	7.508
H_2N-SiH_2 (**15**)	C_s (0)	−345.912871	−346.134048	−346.171658	26.23	0.751	1.356	1.266	1.254	93.24	13.56	12.41
H_2N-H_2-SiH_TS (**16**)	C_1 (1)	−346.419280	−346.660480	−346.704425	30.49		2.271	2.069	2.184	62.82	11.18	10.98
$H_2N-SiH-H_2$ (**17**)	C_1 (0)	−346.485915	−346.712813	−346.758139	28.46		1.996	1.783	1.691	26.07	8.722	7.210
H_2N-SiH (18)	C_s (0)	−345.341466	−345.552088	−345.589322	21.42		2.008	1.799	1.708	138.1	14.79	13.36
$H_2N-H-Si$_TS (**19**)	C_1 (1)	−345.199062	−345.412452	−345.453117	19.89		3.513	3.192	3.828	192.4	11.66	11.39
H_3N-Si (**20**)	C_{3v} (0)	−345.230601	−345.438409	−345.481239	23.90		5.604	5.372	5.605	185.5	9.701	9.689
H_3N-SiH_2_3 (**21**)	C_s (0)	−346.399611	−346.630465	−346.671947	32.49	2.001	1.310	0.156	0.407	71.54	10.27	9.828
H_3N-SiH_2_3_TS (**22**)	C_s (1)	−346.377445	−346.609430	−346.651503	28.02	2.001	2.185	3.164	3.839	66.82	11.56	11.18
$H_2N-H-SiH_2$_3 (**23**)	C_s (0)	−346.411299	−346.633999	−346.671642	26.36	2.001	1.343	1.266	1.253	22.39	12.04	9.079
$H_2N-SiH-H$_TS (**24**)	C_1 (1)	−345.837181	−346.049709	−346.090260	21.91	0.851	2.094	1.906	1.552	51.96	12.64	11.88
$H_2N-SiH-H$ (**25**)	C_1 (0)	−345.839968	−346.051976	−346.089235	21.59	0.750	1.994	1.795	1.702	29.08	11.85	9.494
$H_2N-H-SiH$_TS (**26**)	C_1 (1)	−345.816610	−346.040255	−346.084967	24.30	0.795	2.967	2.743	2.989	98.18	11.94	11.34
H_3N-SiH (**27**)	C_s (0)	−345.875989	−346.095435	−346.137001	28.89	0.760	5.635	5.404	5.535	101.0	9.730	9.323
$HN-H_2-SiH_2$_TS (**28**)	C_1 (1)	−346.396260	−346.637533	−346.676611	27.88		2.043	1.981	2.392	60.86	14.02	13.20
$HN-H_2-SiH_2$ (**29**)	C_1 (0)	−346.462316	−346.689393	−346.730720	26.35		2.824	2.770	3.557	41.08	9.657	7.926
$HN-SiH_2$ (**30**)	C_s (0)	−345.317279	−345.527446	−345.560760	18.74		2.666	2.592	3.357	136.2	16.36	14.60
$HN-H-SiH$_TS (**31**)	C_1 (1)	−345.224463	−345.437352	−345.476105	16.32		1.790	1.629	1.881	124.0	15.73	14.53
H_2N-SiH_3 (**32**)	C_s (0)	−345.281447	−345.490859	−345.523838	20.59	2.001	1.424	1.347	1.331	164.0	13.65	13.56
H_2N-SiH_3_TS (**33**)	C_1 (1)	−345.186135	−345.398422	−345.442338	16.45	2.038	1.564	1.572	1.919	129.1	14.77	14.42
$HN-SiH_2$_3 (**34**)	C_s (0)	−345.240094	−345.448779	−345.490828	17.83	2.005	1.640	1.613	1.816	109.6	13.99	13.48
$N-H_2-SiH$_TS (**35**)	C_1 (1)	−345.156753	−345.373313	−345.402532	14.58		4.525	4.468	5.463	96.82	17.50	14.82
$N-H_2-SiH$ (**36**)	C_1 (0)	−345.231397	−345.434085	−345.455189	13.19		3.954	3.889	6.192	7122	7.521	7.513
HSiN (**37**)	$C_{\infty v}$ (0)	−344.086484	−344.272721	−344.285759	5.88		3.818	3.729	5.964	0.000	17.52	17.52
$H-H_2N-Si$_TS (**38**)	C_1 (1)	−345.169691	−345.379622	−345.480633	17.56		1.695	2.233	4.041	161.3	12.37	12.06
H_2-HNSi (**39**)	C_1 (0)	−345.324853	−345.528820	−345.562223	15.65		0.065	0.184	0.971	38.58	10.49	8.250
HNSi (**40**)	$C_{\infty v}$ (0)	−344.180391	−344.367947	−344.393273	8.61		0.026	0.143	0.930	0.000	18.51	18.51
H_3N-Si_3 (**41**)	C_{3v} (0)	−345.277734	−345.484810	−345.521096	24.24	2.021	5.555	5.327	5.544	184.3	9.413	9.413
$H_2N-H-Si$_3_TS (**42**)	C_s (1)	−345.212611	−345.424568	−345.464801	18.80	2.036	2.932	2.682	3.131	169.6	12.15	12.12
$H-NH_2-Si$_3_TS (**43**)	C_1 (1)	−345.203856	−345.410917	−345.453034	18.76	2.096	2.082	1.882	3.392	161.4	12.42	12.31
$H_2N-Si-H$_3 (**44**)	C_{2v} (0)	−345.234680	−345.434876	-345.467399	15.91	2.008	2.039	1.886	1.826	353.4	8.646	8.440
H_2N-Si (**45**)	C_s (0)	−344.736210	−344.934989	−344.967497	15.79	0.758	2.081	1.877	1.815	353.5	15.03	14.42
$HN-H_2-Si$_TS (**46**)	C_s (1)	−345.235490	−345.456136	−345.490295	16.45		0.713	0.735	0.943	98.27	16.79	14.34
H_2N-H_2-Si_TS (**47**)	C_s (1)	−345.809683	−346.039341	−346.079297	24.45	0.761	2.276	2.075	2.171	85.47	11.77	10.98
$H_2N-Si-H_2$ (**48**)	C_s (0)	−345.880630	−346.095717	−346.136327	22.82	0.758	2.076	1.858	1.797	25.39	10.01	7.481
$HN-Si-H$_TS (**49**)	C_1 (1)	−344.642222	−344.837514	−344.882162	10.35	0.924	1.748	2.423	0.786	253.3	16.76	15.72
$HNSi-H$ (**50**)	C_1 (0)	−344.678832	−344.867797	−344.893138	8.70	0.750	0.058	0.144	0.931	31.82	15.79	10.55
$N-H-Si$_TS (**51**)	C_s (1)	−344.020092	−344.206874	−344.268056	4.81		3.992	3.942	2.534	229.0	21.46	19.62
HNSi_3 (**52**)	C_s (0)	−344.015533	−344.203161	−344.252394	7.21	2.008	2.626	2.647	2.060	1774	18.24	18.05
$N-H-Si$_3_TS (**53**)	C_s (1)	−343.956253	−344.147471	−344.199341	4.45	2.169	2.548	2.646	1.360	326.2	19.34	18.26
HSiN_3 (**54**)	C_s (0)	−344.004666	−344.190416	−344.238691	8.44	2.208	3.113	3.393	2.488	240.7	20.14	18.58
HNSi_3_TS (**55**)	C_s (1)	−343.946641	−344.128704	−344.177404	3.54	2.148	3.849	4.448	3.919	339.1	18.65	17.68
$H-NSi$_3_TS (**56**)	$C_{\infty v}$ (0)	−343.963561	−344.140696	−344.188697	2.23	2.276	3.523	3.627	1.855	0.000	10.57	10.57
NSi (**57**)	$C_{\infty v}$ (0)	−343.465170	−343.640816	−343.688803	2.12	1.026	3.559	3.609	1.847	0.000	22.88	22.88

[a] Symmetry of the species, the number of imaginary frequency are in parentheses. [b] MP2/6-31+G*//MP2/6-31+G* calculations. [c] MP2/6-311++G**//MP2/6-31+G* calculations. [d] CCSD(T)/6-311++G**//MP2/6-31+G* calculations.

We have shown that incorporating triple split basis functions is important to lower the total energies of the species containing silicon.[32] Energies calculated using two different basis sets and theoretical levels were listed together with dipole moments, and rotational constants for all the species in Table 1. For open shell species using spin-unrestricted methods, spin-squared expectation values $\langle S^2 \rangle$ were also listed to assess spin contamination, which are reported as a major source of errors in predicting radical reaction pathways.[40]

The species were named according to their structures and numbered to indicate their order of occurrence in the reaction courses. Symbols "3" or "TS" were added to specify triplet state or transition state species.

Reaction pathways were divided into six parts. Each part includes geometry structures of the relevant species and their energies relative to the initial molecular complex H_3N-SiH_4 (**1**) (Figures 1−6).

Part I: Pathways from SiH_4 + NH_3 to H_2N-SiH_3 (4), H_3N-SiH_2 (6), and H_2N-SiH_2 (15) (Figure 1). Initially, SiH_4 and NH_3 can associate into a molecular complex H_3N-SiH_4 (**1**). Experimental evidence for the existence of **1** and the weak electron donor−acceptor interaction nature of the N−Si bond

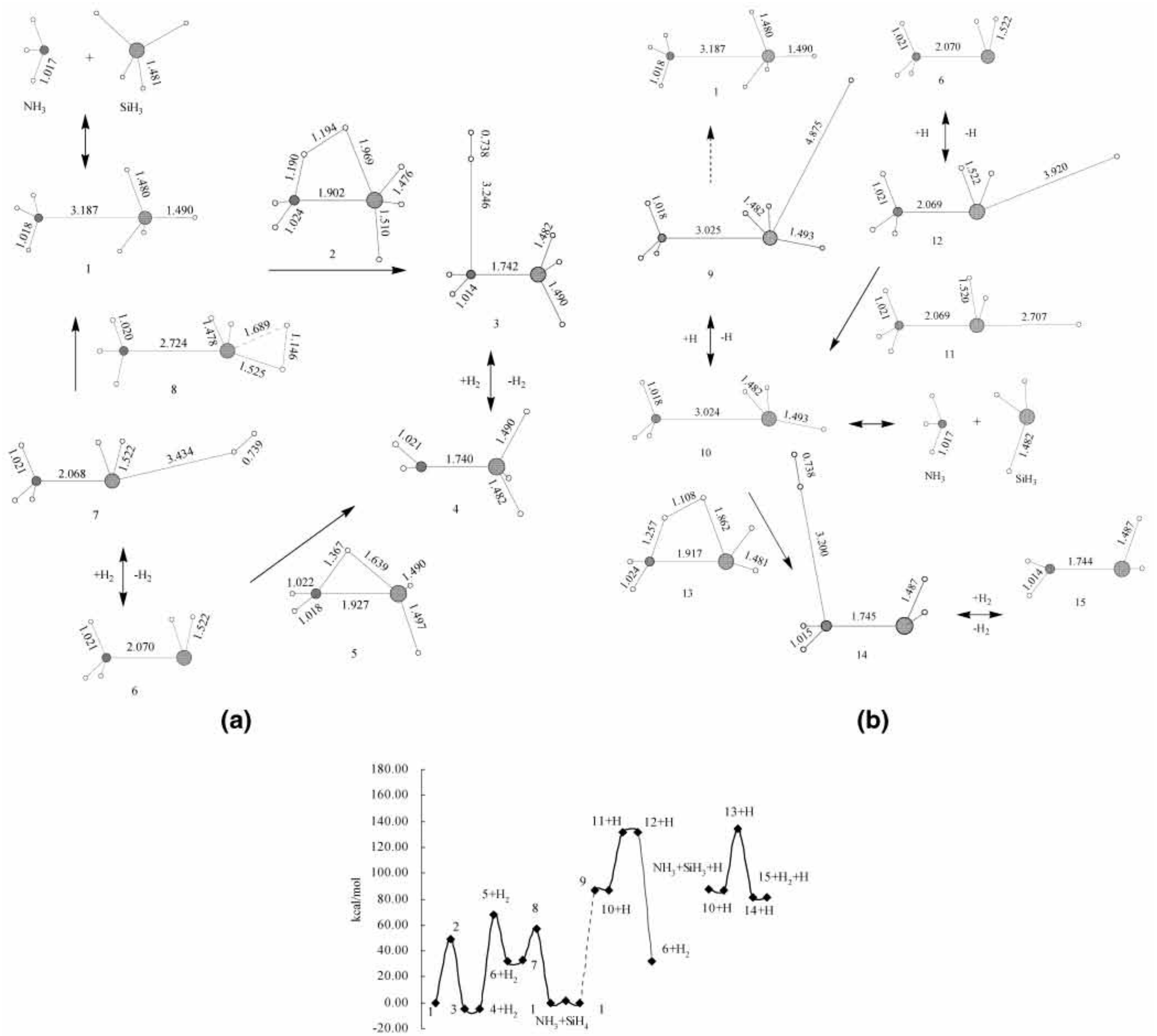

Figure 1. Species involved in hydrogen elimination from H_3N-SiH_4 (**1**). Bond lengths are in Å; the species beside the arrows are transition states, H_2, or H. The direction of the arrows is toward energy descent. The dashed lines or arrows indicate triplet−singlet transitions. The relative energy of H_3N-SiH_4 (**1**) is 0.00 kcal/mol.

have been reported.[3,38] As a result, the two monomers in **1** are more compact than silane dimer SiH_4-SiH_4. The dipole moment of **1** is significantly larger than that of NH_3, indicating the electron flow effect upon NH_3 bonding to SiH_4. With 49.31 kcal/mol energy, the system can be activated to transition state $H_2N-H_2-SiH_3$_TS (**2**). The ring structure of **2** is formed through an intramolecular dihydrogen bond −H−H−, which is responsible for the first H_2 elimination. The direct product is $H_2N-SiH_3-H_2$ (**3**), a molecular combination of silylamine H_2N-SiH_3 (**4**) and H_2. The energy of **3** is −4.55 kcal/mol relative to **1**. Dihydrogen bonding,[41,42] a newly discovered unconventional interaction between two species containing partial oppositely charged hydrogen atoms, has been found responsible for molecule−cation interaction between silane and ammonium.[43] For the neutral SiH_4/NH_3 system, because the N−Si bond is dative in nature, as it shortens, more electrons transfer from nitrogen to silicon, and the more negatively charged hydrogen atom in Si−H then tends to associate with the more positively charged one in N−H. This accounts for the formation of a dihydrogen bond −H−H− in **2**.

The second route is an analogue of H_2 elimination in the pure SiH_4 system. The two H atoms of SiH_4 monomer in **1** associate to H_2, as shown by transition state $H_3N-SiH_2-H_2$_TS (**8**). To activate **1** to **8** requires 57.47 kcal/mol energy, forming a barrier of 8.16 kcal/mol higher than that along the first route. The H_2 then eliminates to produce $H_3N-SiH_2-H_2$ (**7**), a molecular combination of a donor−acceptor complex H_3N-SiH_2 (**6**) and H_2. The energy of **6** is 37.18 kcal/mol relative to **4**. Compared with SiH_4, the electron donor NH_3 can stabilize the remaining SiH_2 more effectively. As a result, the activation energy is slightly lower to produce **6** than to produce the SiH_4-SiH_2 complex. In addition, the transient intermediate SiH_4-SiH_2 isomerizes to normal disilane Si_2H_6 with almost no barrier,[29,30] whereas 35.23 kcal/mol energy is required to turn **6** into the more stable **4**. The transition state for the latter isomerization is $H_2N-H-SiH_2$ (**5**), a hydrogen-bridged structure. Therefore, it is likely that a large amount of **4** is produced along the first rather than the second route, and **6** should be a detectable intermediate species if the activation energy is sufficient to dissociate SiH_4 to SiH_2 and H_2. Compared with **4**, the donor−

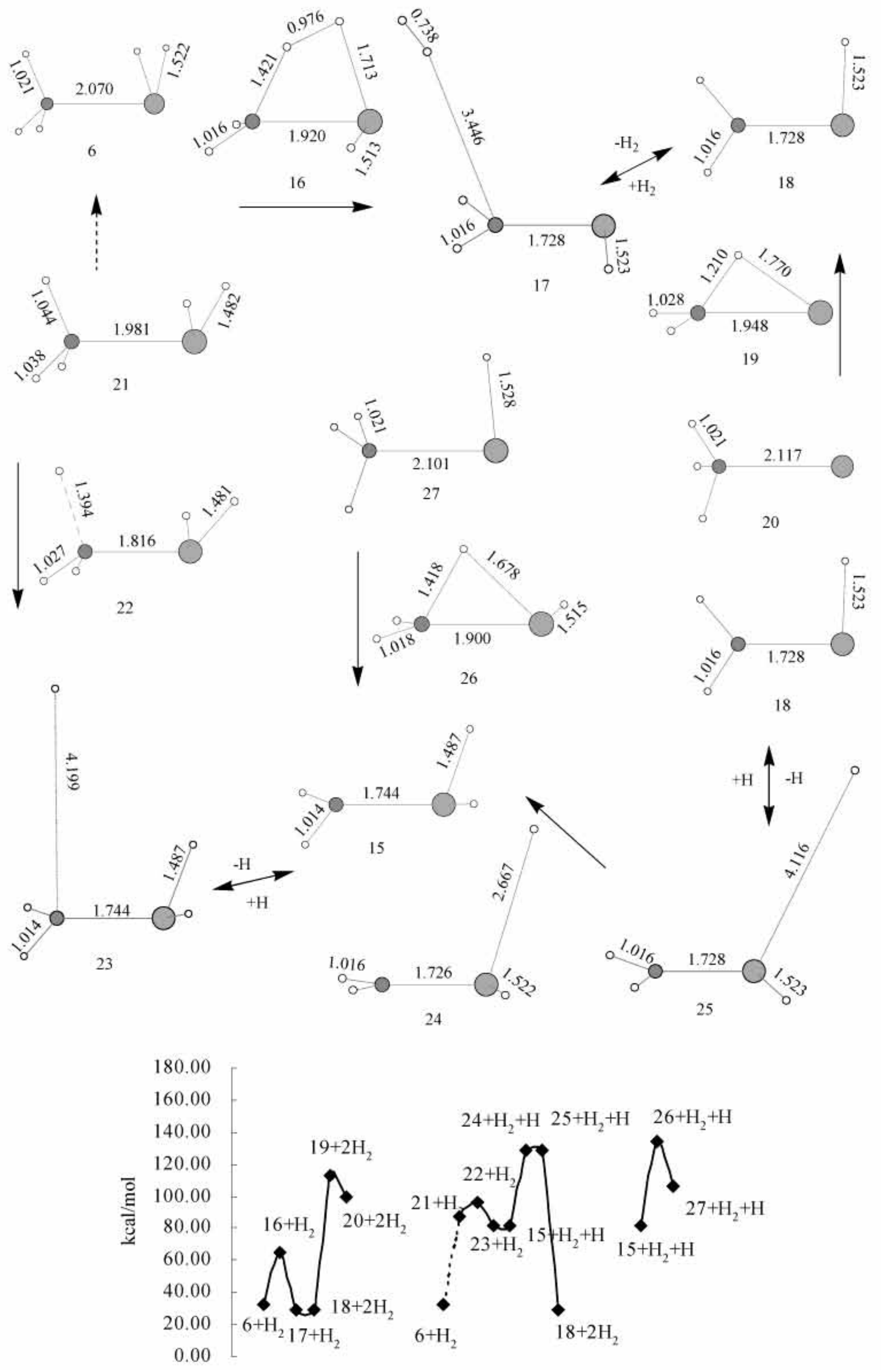

Figure 2. Species involved in hydrogen elimination from H_3N-SiH_2 (**6**). Bond lengths are in Å; the species beside the arrows are transition states, H_2, or H. The direction of the arrows is toward energy descent. The dashed lines or arrows indicate triplet−singlet transitions. The relative energy of H_3N-SiH_4 (**1**) is 0.00 kcal/mol.

acceptor complex **6** is less stable and its dipole moment is much larger. This implies that **6** is more stable under polar conditions and may be easier to condense.

With 87.05 kcal/mol energy, one of the hydrogen atoms attached to silicon in **1** can dissociate as shown by triplet state $H_3N-SiH_3-H\_3$ (**9**), leaving H_3N-SiH_3 (**10**), a loosely bonded complex of NH_3, and the radical SiH_3. Unlike SiH_2, SiH_3 is essentially not stabilized by NH_3. Thus the binding energy is only 0.96 kcal/mol between NH_3 and SiH_3, compared to the binding energy of 22.37 kcal/mol between NH_3 and SiH_2. One of the three Si−H bonds in **10** is longer than the other two, implying that there is the potential for further H elimination. With 44.24 kcal/mol energy, the second H eliminates from **10** through transition state $H_3N-SiH_2-H\_TS$ (**11**) to H_3N-SiH_2-H (**12**). If the second dissociated H then associates with the first one to form H_2, the energy of the total system falls to that of $\mathbf{6} + H_2$. The stepwise H elimination is energy demanding and influenced by the concentration of surrounding atomic H.

H_2 elimination can also take place from radical **10** via a dihydrogen-bonded transition state $H_2N-H_2-SiH_2$_TS (**13**). The activation energy is 47.19 kcal/mol, slightly lower than that from **1** to **2**. The product $H_2N-SiH_2-H_2$ (**14**) is a weak combination of radical H_2N-SiH_2 (**15**) and H_2. The energy of **14** is −5.48 kcal/mol relative to **10**.

For triplet and doublet state species discussed in this part, the calculated $\langle S^2\rangle$ values are close to 2 and 0.75, respectively, indicating small spin contamination.

Part II: Pathways from H_3N-SiH_2 (6) to H_2N-SiH (18), H_3N-Si (20), H_2N-SiH_2 (15), and H_3N-SiH (27) (Figure 2). Because the dative N−Si bond in **6** is stronger than that in **1**, the H atom should be more positively charged in N−H and more negatively charged in Si−H. This presumption is justified by easier formation of another intramolecular dihydrogen-bonded transition state structure H_2N-H_2-SiH_TS (**16**). The activation energy is 32.44 kcal/mol relative to **6**, marking a much lower barrier for second H_2 elimination from **6**. The product $H_2N-SiH-H_2$ (**17**), a molecular combination of H_2N-SiH (**18**) and H_2, is 3.30 kcal/mol more stable than **6**. Compound **18** can be seen either as a −SiH derivative of NH_3 or as a $-NH_2$ derivative of SiH_2, but the atoms are confined in one plane and the dipole moment of **18** is larger than that of NH_3, indicating the electron delocalization effect on the geometry. With 83.93 kcal/mol activation energy, the H attached to silicon in **18** can transfer to nitrogen, as shown by transition state $H_2N-H-Si$_TS (**19**). This process results in H_3N-Si (**20**), a complex formed between NH_3 and silicon. The energy of **20** is 70.30 kcal/mol relative to **18**. The dipole moment of **20** is much larger than **18**, indicating **20** is an electron donor−acceptor complex.

With 87.24 kcal/mol energy to the system, the singlet ground electronic state of **6** can be activated to triplet state H_3N-SiH_2_3 (**21**). The energy gap between the two states is 54.82 kcal/mol. The structural change from **6** to **21** is small, but the dipole moment drops significantly. Over a small barrier (8.36 kcal/mol) through triplet transition state H_3N-SiH_2_3_TS (**22**), one of the N−H bond breaks and results in $H_2N-H-SiH_2$_3 (**23**), a weak combination of radical **15** and H atom. The three triplet state species involved in the reaction all have correct $\langle S^2\rangle$ values. Over a barrier of 46.75 kcal/mol, the SiH_3 like radical **15** can dissociate another H as shown by transition state $H_2N-SiH-H$_TS (**24**) and produce $H_2N-SiH-H$ (**25**). If dissociated H combines with another H into H_2, the system falls to **18** and two H_2 molecules. Clearly, the atomic stepwise transformation from **6** to **18** is much more energy demanding. In calculating the doublet transition state **24**, spin contamination appears serious, with an $\langle S^2\rangle$ value larger than 0.8, but the geometry and energy of **24** are very close to **25**, which has a correct $\langle S^2\rangle$ value.

Another energy-rising process leading **15** to H_3N-SiH (**27**) is via H-bridged transition state $H_2N-H-SiH$_TS (**26**). The barrier is 52.47 kcal/mol and the energy of **27** is 24.40 kcal/mol relative to **15**. The spin contaminations of the three species are all small. It seems that large spin contamination is likely to happen when a loosely bonded radical transition state such as **24** is evaluated, which can be seen as a molecule−radical complex, whereas for a compact doublet transition state such as **26**, the spin contamination is less serious.

In summary, a H_2 molecule is most easy to dissociate from **6**, resulting in a more stable product **18**. Probably this is the reason that the predicted intermediate species **6** is not easily observed.

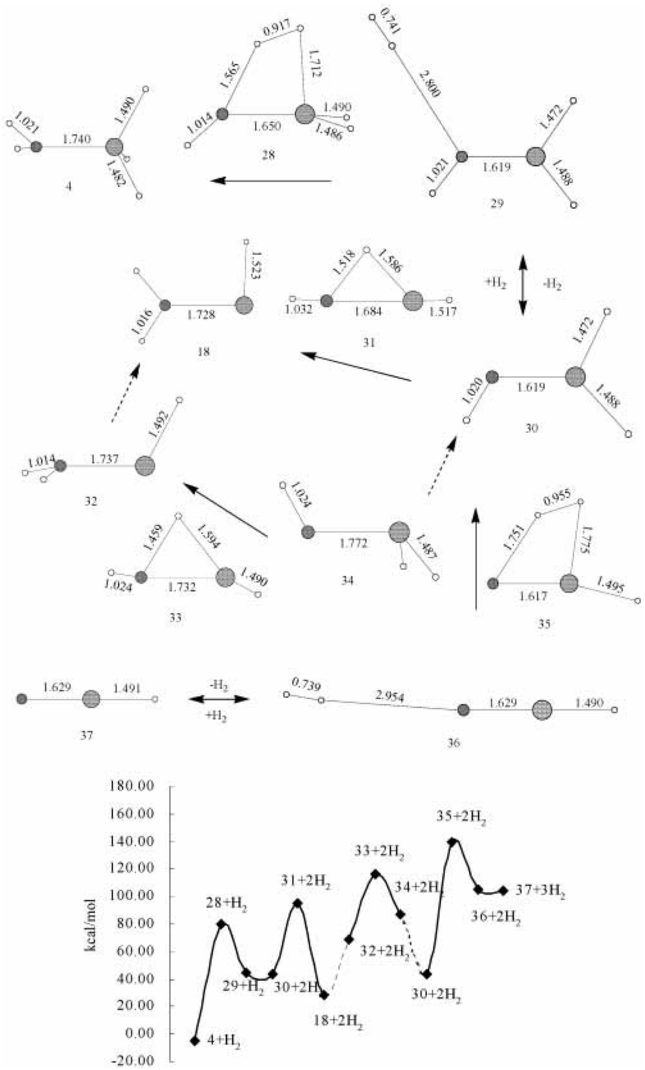

Figure 3. Species involved in hydrogen elimination from H_2N-SiH_3 (**4**). Bond lengths are in Å; the species beside the arrows are transition states, H_2, or H. The direction of the arrows is toward energy descent. The dashed lines or arrows indicate triplet−singlet transitions. The relative energy of H_3N-SiH_4 (**1**) is 0.00 kcal/mol.

Part III: Pathways from H_2N-SiH_3 (4) to $HN-SiH_2$ (30), H_2N-SiH (18), and HSiN (37) (Figure 3). With 84.46 kcal/mol activation energy, a dihydrogen-bonded ring structure can also be formed from species **4**, as shown by transition state $HN-H_2-SiH_2$ (**28**). Because the N−Si bond in **4** is covalent rather than dative in nature, the smaller electronic transfer effect accounts for the 52.02 kcal/mol higher barrier from **4** to $HN-SiH_2-H_2$ (**29**) than that from **6** through **16** to **17**. Compared with **17**, the eliminating H_2 connects a little more closely to nitrogen in **29**. The silicon in the H_2-eliminated product $HN-SiH_2$ (**30**) is three-coordinated with a planar structure, indicating the N−Si bond has some double bond character. The energy of **30** is 15.24 kcal/mol relative to the most stable three-hydrogen isomer **18**. One H atom has to transfer between nitrogen and silicon, leading to interconversion of **30** and **18**. Such conversion can be realized through either a singlet or triplet state. To activate **18** to transition state $HN-H-SiH$_TS (**31**) requires 65.94 kcal/mol energy. Alternatively, with 25.01 kcal/mol energy, compound **18** can be excited to triplet state $HN-SiH_2$_3 (**32**), which then transfers a H atom from silicon to nitrogen through triplet transition state $HN-H-SiH$_3_TS (**33**), resulting in H_2N-SiH_3 (**34**), the triplet state of **30**. The barrier is 47.00 kcal/mol relative to **32**. The energy of **34** is 42.98 kcal/mol relative to **30**. Unlike the planar structure of the low spin species **18** and **30**, the H atoms in the high spin species **32** and **34** are

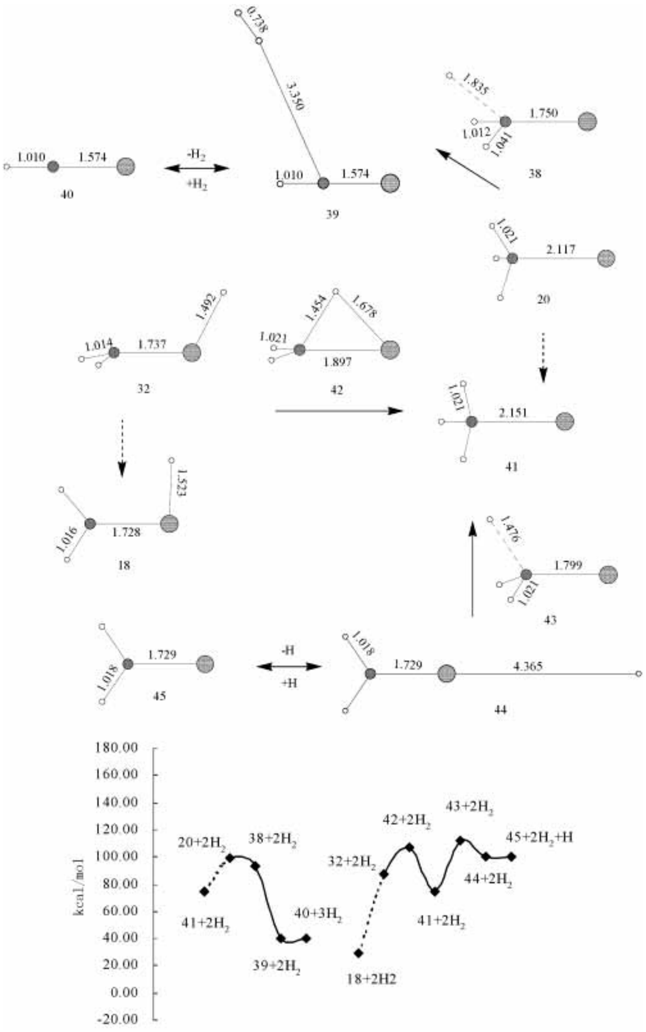

Figure 4. Species involved in isomerization and hydrogen elimination from $H_3N{-}Si$ (**20**). Bond lengths are in Å; the species beside the arrows are transition states, H_2, or H. The direction of the arrows is toward energy descent. The dashed lines or arrows indicate triplet−singlet transitions. The relative energy of $NH_3{-}SiH_4$ (**1**) is 0.00 kcal/mol.

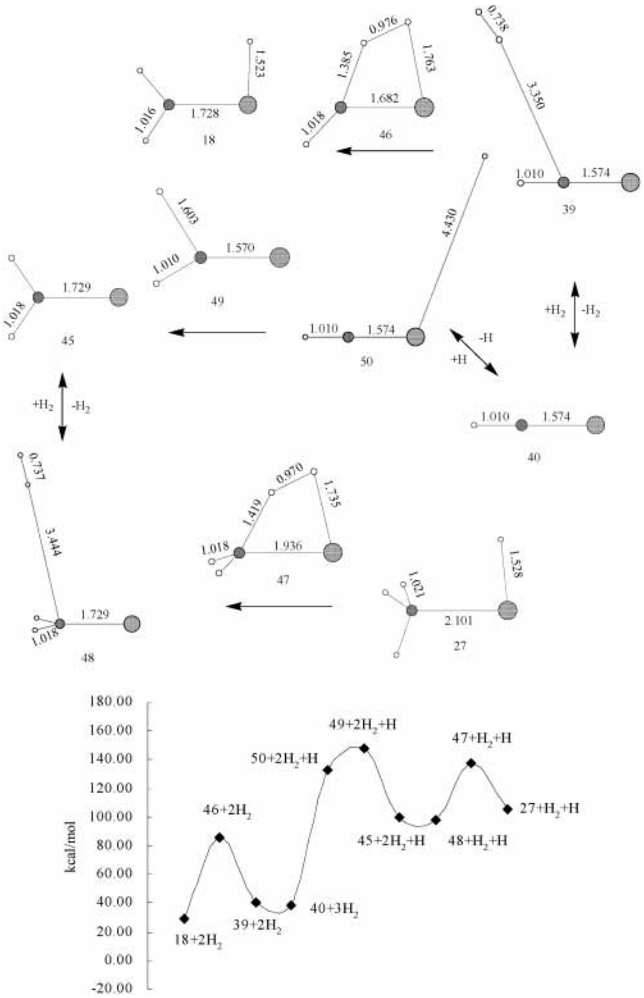

Figure 5. Species involved in hydrogen elimination from $H_2N{-}SiH$ (**18**) and $H_3N{-}SiH$ (**27**). Bond lengths are in Å; the species beside the arrows are transition states, H_2, or H. The direction of the arrows is toward energy descent. The dashed lines or arrows indicate triplet−singlet transitions. The relative energy of $H_3N{-}SiH_4$ (**1**) is 0.00 kcal/mol.

not confined in the molecular plane but prefer staggered positions, showing single bond characteristics. The calculated $\langle S^2\rangle$ values of the three triplet state species are all close to 2, indicating small spin contamination.

Providing 95.13 kcal/mol energy to **30**, the H in N−H can associate with the H in Si−H to form another dihydrogen-bonded transition state $N{-}H_2{-}SiH\_TS$ (**35**). The H_2 elimination results in $HSiN{-}H_2$ (**36**), a molecular combination of HSiN (**37**) and H_2. The energy of **36** is 60.69 kcal/mol relative to **30**.

Part IV: Pathways from $H_3N{-}Si$ (20) to $H_2N{-}SiH$ (18), $H_3N{-}Si\_3$ (41), HNSi (40), and $H_2N{-}Si$ (45) (Figure 4). The structure of **20** shows it is like a molecule-radical complex formed between the NH_3 and Si atoms. The ground state of this complex is not the singlet state **20**, but the triplet state $H_3N{-}Si\_3$ (**41**). From **20** to **41**, the energy gap is 24.67 kcal/mol. But the structures of the two states are quite similar. The pathways started from **20** or **41** represent the molecule−atom reactions between the NH_3 and Si atoms, which has been recently studied both experimentally and theoretically.[6] At triplet state, one of the H connected to nitrogen transfers to silicon through a bridged transition state $H_2N{-}H{-}Si\_3\_TS$ (**42**), resulting in **32**, the triplet state of **18**. The barrier of the process is 29.89 kcal/mol relative to **41**. Alternatively, one of the H connected to nitrogen can dissociate from **41**, as shown by transition state $H{-}H_2N{-}Si\_3\_TS$ (**43**), resulting in $H{-}H_2N{-}Si\_3$ (**44**), a loose combination of H and radical $H_2N{-}Si$ (**45**). The barrier of the process is 37.23 kcal/mol and the energy of product **44** is 25.37 kcal/mol relative to **41**. Therefore, for **41**, it is slightly more energy demanding to produce radical **45** than isomerize to **32**, which can drop to the more stable singlet molecule **18**.

When the open shell species involved in this part is calculated, no serious spin contamination happens.

Hydrogen elimination can take place from singlet state **20**. As shown by transition state $H{-}H_2N{-}Si\_TS$ (**38**) and product $H_2{-}HNSi$ (**39**), one of the H atoms dissociates first, which then abstracts another H, leading to a H_2 molecule. When the energy of **38** is calculated, however, large discrepancies appear when different methods are used. At MP2 level, the energy of **38** is more than 30 kcal/mol higher than that of **20**, whereas the barrier almost disappears when the CCSD(T) method is used. More investigation and experimental evidence are necessary to clarify the situation. Nevertheless, the H_2 elimination results in a linear molecule HNSi (**40**). The energy of **39** is −34.40 kcal/mol relative to **41**, indicating **40** is quite a stable product resulting from interaction between silicon atom and ammonia.

Part V: Pathways from $H_2N{-}SiH$ (18) to HNSi (40), $H_3N{-}SiH$ (27) to $H_2N{-}SiH$ (45) and HNSi (40) (Figure 5).

The third H_2 elimination from the total system can also be realized through intramolecular dihydrogen-bonded transition state HN−H_2−Si_TS (**46**); each H of the −H−H− bond comes from the N−H and Si−H bonds in **18**. To activate **18** to **46** requires 57.17 kcal/mol energy, larger than the energy rise in first and second H_2 eliminations. The product is **39**, a molecular combination of **40** and H_2, same as the H_2-eliminated product of **20**.

Started from intermediate radical **27**, H_2 elimination can also take place through dihydrogen-bonded transition state H_2N−H_2−Si_TS (**47**), resulting in H_2N−Si−H_2 (**48**), a radical−molecule combination of **45** and H_2. Relative to **27**, the barrier of the process is 31.78 kcal/mol and the energy of the product **48** is −5.64 kcal/mol, indicating **45** is a more stable radical than **27**. Over a barrier of 48.11 kcal/mol, a H atom can dissociate from **45**, as shown by transition state HN−Si−H_TS (**49**) and product HNSi−H (**50**), a weak combination of molecule **40** and H atom. As the two H atoms associate into H_2, the system's total energy falls to that of **40** plus three H_2. When the radical species involved in this part is calculated, serious spin contamination happens in the doublet transition state **49**. Unlike radical **47**, another doublet transition state, the structure of **49** is more like a molecule−radical complex. It seems spin contamination is likely to happen when such transition states are calculated.

Among the various ways toward **40**, the smallest molecule produced from the $SiH_4/NH_3 = 1:1$ system through hydrogen elimination, the route **1** → **6** → **18** → **40** is least energy demanding. Two dihydrogen-bonded transition states **16** and **46** are responsible for lowering the barriers from **6** to **18** and from **18** to **40**.

Part VI: Pathways from HNSi (40) to HSiN (37) and NSi (57) (Figure 6). Molecule **40** is 64.73 kcal/mol more stable than its isomer **37**, different from their carbon analogues, for which HCN is more stable than HNC. Over a barrier of 10.04 kcal/mol, the less stable isomer **37** can transform to **40** with the H migrating from nitrogen to silicon, as shown by the transition state N−H−Si_TS (**51**). The isomerization can also happen at the triplet state. With 87.01 kcal/mol energy, the singlet−triplet transition can happen from **40** to HNSi_3 (**52**). Much less energy (32.09 kcal/mol) is required to excite **37** to its triplet state HSiN_3 (**54**). As a result, the two species are energetically closer at triplet states than at singlet states. Exciting from singlet to triplet state, the structure of both species changes from linear to bent, indicating that the two unpaired electrons may localize on nitrogen and silicon separately. The interconversion between **52** and **54** can be realized through H transfer between nitrogen and silicon, as shown by transition state N−H−Si_3_TS (**53**). The barrier of this process is 20.70 kcal/mol relative to **54**.

Providing 43.38 kcal/mol energy to **52**, the H attached to nitrogen can dissociate as shown by transition state **55**, resulting in H−NSi_3_TS (**56**), a loose combination of radical NSi (**57**) and the dissociated H atom. The energy of **56** is 34.99 kcal/mol relative to that of **52**. The small barrier shows some potential that the radical NSi can be detected. With the small radical NSi, the systems total energy reaches to 170.30 kcal/mol relative to **1**. It seems that H dissociation from silicon can also happen in **54**. But the attempt to locate the possible transition state was unsuccessful.

Except for **52**, considerable spin contamination happens when the triplet and doublet species in this part are calculated. Further investigations are necessary to know how much the spin contamination affects the calculated geometry structures and energies.

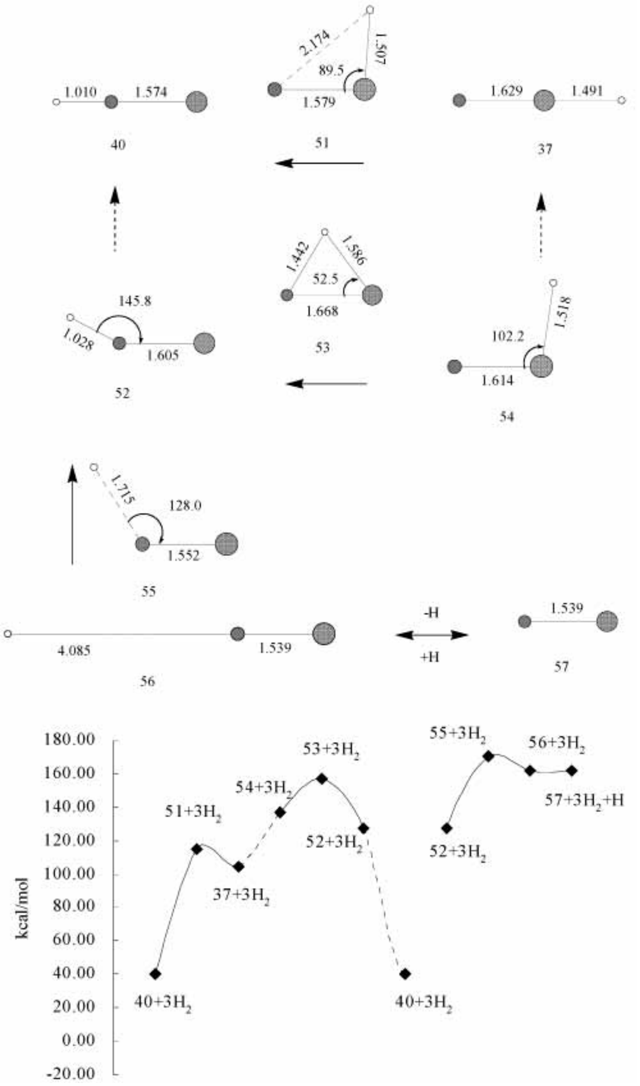

Figure 6. Species involved in isomerization and hydrogen elimination from HNSi (**40**). Bond lengths are in Å; the species beside the arrows are transition states, H_2, or H. The direction of the arrows is toward energy descent; the dashed lines or arrows indicate triplet−singlet transitions; the relative energy of H_3N-SiH_4 (**1**) is 0.00 kcal/mol.

IV. Concluding Remarks

Gas-phase reactions of SiH_4 and NH_3 produce a series of hydrogen-eliminated species containing a N−Si covalent or dative bond. Among them, silylamine H_2N-SiH_3 (**4**) is thermodynamically most stable and kinetically easiest to obtain. The NH_2 derivative of silylene H_2N-SiH (**18**) is the most stable isomer after second H_2 elimination. The linear molecule HNSi (**40**) is the most stable isomer after third H_2 elimination. Other products, including molecules H_3N-SiH_2 (**6**), H_3N-Si (**20**), HN−SiH_2 (**30**), and HSiN (**37**), radicals H_2N-SiH_2 (**15**), H_3N-SiH (**27**), H_2N-Si (**45**), and NSi (**57**) can be produced as transient intermediates via H_2 or H elimination or isomerization at various stages. Dihydrogen bonding, appearing in several transition state structures, is found to be responsible for H_2 elimination along pathways with relatively low activation energy. The atomic H elimination involving singlet−triplet excitation, with radicals as intermediates, requires higher activation energy.

References and Notes

(1) O'Neal, H. E.; Ring, M. A.; Martin, J. G.; Navio, M. T. *J. Phys. Chem. A* **1998**, *102*, 8493.

(2) Melius, C. F.; Ho, P. *J. Phys. Chem.* **1991**, *95*, 1410.

(3) Meininger, D. R.; Ault, B. S. *J. Phys. Chem. A* **2000**, *104*, 3481.

(4) Schmidt, M. W.; Windus, T. L.; Gordon, M. S. *J. Am. Chem. Soc.* **1995**, *117*, 7480.

(5) Korkin, A. A.; Cole, J. V.; Sengupta, D.; Adams, J. B. *J. Electrochem. Soc.* **1999**, *146*, 4203.

(6) Chen, M. H.; Zheng, A. H.; Lu, H.; Zhou, M. F. *J. Phys. Chem. A* **2002**, *106*, 3077.

(7) Yacoubi, K.; Azzaro-Pantel, C.; Scheid, E.; Couderc, J. P. *J. Electrochem. Soc.* **1999**, *146*, 3009.

(8) Yacoubi, K.; Azzaro-Pantel, C.; Couderc, J. P. *J. Electrochem. Soc.* **1999**, *146*, 3018.

(9) Himmel, H. J.; Schiefenhovel, N.; Binnewies, M. *Chem-Eur. J.* **2003**, *9*, 1387.

(10) Ohta, H.; Nagashima, A.; Hori, M.; Goto, T. *J. Appl. Phys.* **2001**, *89*, 5083.

(11) Yoshimoto, M.; Takubo, K.; Ohtsuki, T.; Komoda, M.; Matsunami, H. *J. Electrochem. Soc.* **1995**, *142*, 1976.

(12) Murley, D. T.; Gibson, R. A. G.; Dunnett, B.; Goodyear, A.; French, I. D. *J. Non-Cryst. Solids* **1995**, 187, 324.

(13) Ignatyev, I. S.; Schaefer, H. F. *J. Phys. Chem. A* **2001**, *105*, 7665.

(14) Krempp, M.; Damrauer, R. *Organometallics* **1995**, *14*, 170.

(15) Boehme, C.; Lucovsky, G. *J. Appl. Phys.* **2000**, *88*, 6055.

(16) Stannowski, B.; Rath, J. K.; Schropp, R. E. I. *J. Appl. Phys.* **2003**, *93*, 2618.

(17) Patil, S. B.; Kumbhar, A.; Waghmare, P.; Rao, V. R.; Dusane, R. O. *Thin Solid Films* **2001**, *395*, 270.

(18) Boehme, C.; Lucovsky, G. *J. Vac. Sci. Technol. A* **2001**, *19*, 2622.

(19) Gleskova, H.; Wagner, S.; Gasparik, V.; Kovac, P. *Appl. Surf. Sci.* **2001**, *175*, 12.

(20) Santana, G.; Morales-Acevedo, A. *Sol. Energ. Mat. Sol. C* **2000**, *60*, 135.

(21) Ghosh, S.; Dutta, P. K.; Bose, D. N. *Mater. Sci. Semicon. Proc.* **1999**, *2*, 1.

(22) Sahu, S.; Kavecky, S.; Szepvolgyi, J. *J. Eur. Ceram. Soc.* **1995**, *15*, 1071.

(23) Riedel, R.; Kleebe, H. J.; Schonfelder, H.; Aldinger, F. *Nature* **1995**, *374*, 526.

(24) Chen, I. W.; Rosenflanz, A. *Nature* **1997**, *389*, 701.

(25) Vashishta, P.; Kalia, R. K.; Ebbsjo, I. *Phys. Rev. Lett.* **1995**, *75*, 858.

(26) Zerr, A.; Miehe, G.; Serghiou, G.; Schwarz, M.; Kroke, E.; Riedel, R.; Fuess, H.; Kroll, P.; Boehler, R. *Nature* **1999**, *400*, 340.

(27) Raghavachari, K.; Chandrasekhar, J.; Gordon, M. S.; Dykema, K. J. *J. Am. Chem. Soc.* **1984**, *106*, 5853.

(28) Jasinski, J. M.; Becerra, R.; Walsh, R. *Chem. Rev.* **1995**, *95*, 1203.

(29) Swihart, M. T.; Girshick, S. L. *J. Phys. Chem. B* **1999**, *103*, 64.

(30) Hu, S. W.; Wang, Y.; Wang, X. Y. Chu, T. W. Liu, X. Q. *J. Phys. Chem. A* **2003**, *107*, 2954.

(31) Hu, S. W.; Wang, Y.; Wang, X. Y. *J. Phys. Chem. A* **2003**, *107*, 1635.

(32) Hu, S. W.; Wang, X. Y. *J. Phys. Chem. A* **2002**, *106*, 9558.

(33) Hu, S. W.; Kim, J.; Tarakeshwar, P.; Kim, K. S. *J. Phys. Chem. A* **2002**, *106*, 6817.

(34) Peng, C. Y.; Ayala, P. Y.; Schlegel, H. B.; Frisch, M. J. *J. Comput. Chem.* **1996**, *17*, 49.

(35) Frisch, M. J.; Trucks, G. W.; Schlegel, H. B.; Scuseria, G. E.; Robb, M. A.; Cheeseman, J. R.; Zakrzewski, V. G.; Montgomery, J. A., Jr.; Stratmann, R. E.; Burant, J. C.; Dapprich, S.; Millam, J. M.; Daniels, A. D.; Kudin, K. N.; Strain, M. C.; Farkas, O.; Tomasi, J.; Barone, V.; Cossi, M.; Cammi, R.; Mennucci, B.; Pomelli, C.; Adamo, C.; Clifford, S.; Ochterski, J.; Petersson, G. A.; Ayala, P. Y.; Cui, Q.; Morokuma, K.; Malick, D. K.; Rabuck, A. D.; Raghavachari, K.; Foresman, J. B.; Cioslowski, J.; Ortiz, J. V.; Stefanov, B. B.; Liu, G.; Liashenko, A.; Piskorz, P.; Komaromi, I.; Gomperts, R.; Martin, R. L.; Fox, D. J.; Keith, T.; Al-Laham, M. A.; Peng, C. Y.; Nanayakkara, A.; Gonzalez, C.; Challacombe, M.; Gill, P. M. W.; Johnson, B. G.; Chen, W.; Wong, M. W.; Andres, J. L.; Head-Gordon, M.; Replogle, E. S.; Pople, J. A. *Gaussian 9*8, revision A.7; Gaussian, Inc.: Frisch, M. J. Pittsburgh, PA, 1998.

(36) Maier, G.; Glatthaar, J. *Angew. Chem., Int. Ed. Engl.* **199**4, *33*, 473.

(37) Maier, G.; Reisenauer, H. P.; Glatthaar, J. *Organometallics* **2000**, *19*, 4775.

(38) Anglada, J. M.; Bo, C.; Bofill, J. M.; Crehuet, R.; Poblet, J. M. *Organometallics* **1999**, *18*, 5584.

(39) Kwon, O.; Kwon, Y. *J. Mol. Struct. (THEOCHEM)* **1999**, *460*, 213.

(40) Wong, M. W.; Radom, L. *J. Phys. Chem.* **1995**, *99*, 8582.

(41) Crabtree, R. H.; Siegbahn, P. E. M.; Eisenstein, O.; Rheingold, A. L. *Acc. Chem. Res.* **1996**, *29*, 348.

(42) Custelcean, R.; Jackson, J. E. *Chem. Rev.* **2001**, *101*, 1963.

(43) Zhu, W. L.; Puah, C. M.; Tan, X. J.; Jiang, H. L.; Chen, K. X. *J. Phys. Chem. A* **2001**, *105*, 426.